Theor Chem Acc (2012) 131:1206
DOI 10.1007/s00214-012-1206-y

REGULAR ARTICLE

# Effect of monomeric sequence on transport properties of D-glucose and ascorbic acid in poly(VP-*co*-HEMA) hydrogels with various water contents: molecular dynamics simulation approach

**Seung Geol Lee · Wonsang Koh · Giuseppe F. Brunello · Ji Il Choi · David G. Bucknall · Seung Soon Jang**

Received: 23 November 2011 / Accepted: 13 March 2012 / Published online: 31 March 2012


**Abstract** We have used full-atomistic molecular dynamics (MD) simulations of both random and blocky sequence hydrogel networks of poly(N-vinyl-2-pyrrolidone-*co*-2-hydroxyethyl methacrylate) (P(VP-*co*-HEMA)) with a composition of VP/HEMA = 37:13 to investigate the effect of the monomeric sequence and the water content on the transport properties of ascorbic acid and D-glucose at 310.15 K. The degrees of randomness of the monomer sequence for the random and the blocky copolymers were 1.170 and 0.104, respectively, and the degree of polymerization was fixed at 50. By analyzing the pair correlation functions, it was found that for both monomeric sequences, the guest molecules (i.e., ascorbic acid and D-glucose) have greater accessibility to the VP units than to the HEMA units due to the higher hydrophilicity of VP compared to HEMA units. While the monomeric sequence effect on the P(VP-*co*-HEMA) hydrogel is clearly observed with 20 wt. % water content, the effect is significantly reduced with 40 wt. % water content and disappears completely with 80 wt. % water content. This is because the hydrophilic guest molecules are more likely to be associated with water molecules than with the polymer network at the high water content. By analyzing the diffusion of the guest molecules and the inner-surface area, it is also found that the guest molecules are confined in the system at 20 wt. % water content, resulting in highly anomalous sub-diffusion. Therefore, at low water content, the diffusion of the guest molecules in the hydrogel is directly affected by the monomeric sequence through the interaction of guest molecules with the monomeric units, whereas such monomeric sequence effects are significantly reduced with increasing water content.

**Keywords** Molecular dynamics simulation · Hydrogels · VP-*co*-HEMA · Ascorbic acid · D-glucose · Monomeric sequence · Transport property

S. G. Lee · G. F. Brunello · J. I. Choi · D. G. Bucknall · S. S. Jang (✉)
School of Materials Science and Engineering, Georgia Institute of Technology, 771 Ferst Drive NW, Atlanta, GA 30332-0245, USA
e-mail: SeungSoon.Jang@mse.gatech.edu

*Present Address:*
S. G. Lee
Materials and Process Simulation Center MC 139-74, California Institute of Technology, Pasadena, CA 91125, USA

W. Koh
School of Physics, Georgia Institute of Technology, 837 State Street, Atlanta, GA 30332-0430, USA

## 1 Introduction

By definition, a hydrogel is a three-dimensionally cross-linked polymeric network that is capable of absorbing and retaining huge amounts of water or biological fluids [1]. Since Wichterle and Lim [2] developed hydrophilic gels for biological use in the early 1960s, significant efforts have been devoted to use the hydrogels in the biomedical and pharmaceutical applications [3, 4], especially for drug delivery and tissue engineering applications due to an excellent biocompatibility and smart stimulus-response properties. Indeed, in order to comply with rapidly increasing demands in medical treatment and health care, a variety of hydrogels have been made and tested so far on the basis of recent progress in organic synthesis techniques that can realize exactly tailored molecular architectures [5, 6].

Poly(2-hydroxyethyl methacrylate) (PHEMA) is one of the most important synthetic hydrogels and has been extensively developed for biomedical applications [7] due

to its nontoxicity, hydrophilicity, biocompatibility, thermal stability, inertness toward many chemicals, high resistance to degradation, and adequate mechanical strength [8]. In addition, PHEMA can be easily polymerized and cross-linked for the fabrication of various architectures [9, 10]. Such properties make PHEMA gel a suitable material for controlled drug release systems [11–15] and for other biomedical and pharmaceutical applications such as artificial skin [16, 17], wound dressing [18, 19], ocular biomaterials [20, 21], and biosensors [22]. Another point we need to stress is that HEMA monomers (Fig. 1a) can be copolymerized with a wide range of other monomers to manipulate their properties. This copolymerization provides an excellent route to control physical properties such as hydrophilicity, solubility, and mechanical strength. Of the various monomers, we are specifically interested in hydrogels of N-vinyl-2-pyrrolidone (VP) (Fig. 1b) copolymerized with HEMA. This is because poly(N-vinyl-2-pyrrolidone-*co*-2-hydroxyethyl methacrylate) (P(VP-*co*-HEMA)) is a well-known, biocompatible hydrogel with a broad range of applications in the biomedical field [23–25], and most importantly, the properties of P(VP-*co*-HEMA) can be tuned for specific applications by adjusting VP/HEMA compositions [26–32]. Moreover, P(VP-*co*-HEMA) hydrogel is one of the major synthetic polymers that has been approved by the Food and Drug Administration (FDA) [33] for medical and pharmaceutical applications. Thus, P(VP-*co*-HEMA) has been extensively studied in biomedical and pharmaceutical applications such as implants for bone substitutes [34], bone tissue regeneration [35], controlled drug delivery [36–38], contact lenses [39, 40], and tissue expanders for reconstructive plastic surgery [41–44].

On the other hand, it should be noted that the physical properties of a copolymer hydrogel system are a function of the distribution of monomer units in the copolymer chain [27, 45]. In other words, the physical properties can be regulated by the microstructural distribution of the monomeric units along the copolymer chains, which depend mainly upon the initial composition of the reaction medium and the reactivity ratio of the monomers participating in the copolymerization reactions [46–48]. Different reactivity ratios of the participating monomers could also affect the formation of the microstructural distribution of the monomeric units during the reaction. In a limiting case, the formation of blocks of the monomer could be expected [49–51]. The reactivity ratios of VP (0.02–0.10) and HEMA (2.97–8.18) monomers have been published by several experimental groups [45, 52]. Because of the significant difference in the reactivity between VP and HEMA, the consumption of HEMA is faster than that of VP during polymerization, which leads to compositional heterogeneity in the copolymer chains [53] and a broad microstructural distribution [27]. Indeed, it was reported from our previous study [54] that the mechanical properties of P(VP-*co*-HEMA) hydrogel depend on the monomeric sequence of P(VP-*co*-HEMA), and the VP monomers (especially in a blocky sequence) are responsible for stress relaxation.

However, despite the intensive effort dedicated to the P(VP-*co*-HEMA) hydrogel, there has been no systematic study to understand how such monomeric sequences affect the transport properties of the hydrogel at a molecular level. Therefore, our primary objective in this study is to elucidate the effect of the monomeric sequence on the transport properties of P(VP-*co*-HEMA) hydrogel with various water contents. For this, we simulated the blocky and random P(VP-*co*-HEMA) hydrogel systems as reported in our previous studies [54, 55] with guest molecules of D-glucose and ascorbic acid (Fig. 1h, i). These were chosen as model guest molecules not only because they are important molecules for their essential role in our body but also because they have very similar size and atomic constituents. Thus, we expect that studying the diffusion of these two similar guest molecules will shed light on our understanding of how the diffusion of guest molecules in hydrogels is affected by the guest–hydrogel molecular interaction that is specified by the structures. For this, full-atomistic MD simulations have been performed to investigate the detailed structure and transport properties of guest molecules through the sequence-dependent structures of the hydrogel.

## 2 Models and simulation details

Full-atomistic MD simulations are performed using two different structural forms of the hydrogel: One is made of a blocky sequence P(VP-*co*-HEMA) (Fig. 1c), and another is made of a random sequence P(VP-*co*-HEMA) (Fig. 1d). The monomeric sequences in our models are intentionally designed to have either a blocky sequence with a degree of randomness (DR) of 0.104 or a random sequence with a DR of 1.170. The value of DR is calculated using the following formula:

$$\mathrm{DR} = \frac{1}{\bar{L}_A} + \frac{1}{\bar{L}_B} \tag{1}$$

where $\bar{L}_A$ and $\bar{L}_B$ are the average number of $A$ or $B$ monomers, respectively, within any one block or segment. From this definition, DR values of 0, 1, and 2 represent homopolymer, fully random copolymer, and alternating copolymer, respectively. All of the chains in our model hydrogel have the same degree of polymerization (DP = 50) and the same composition (VP/HEMA = 37:13). The monomeric composition was chosen to match the composition that was studied experimentally [56]. An

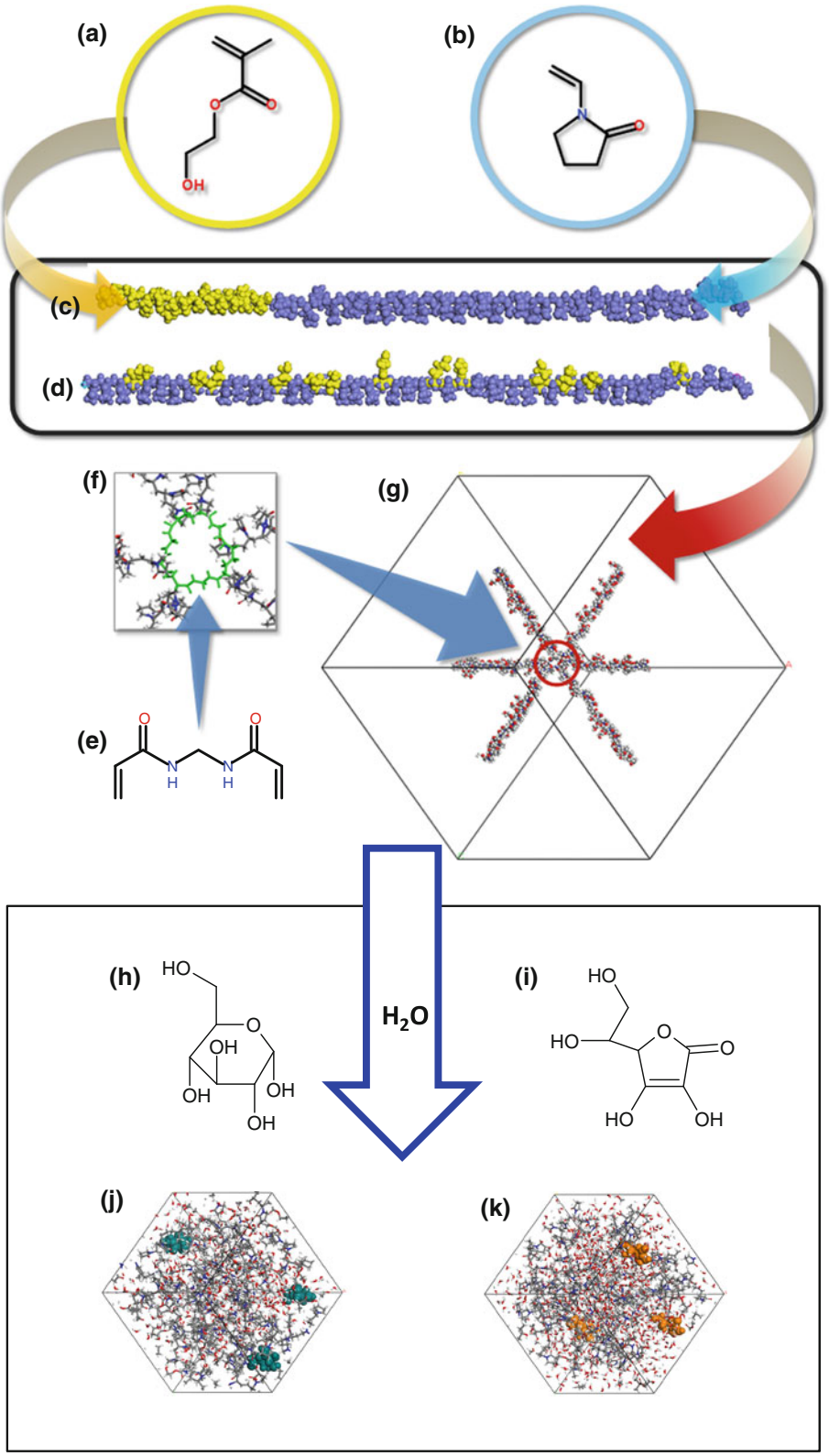


**Fig. 1** Preparation scheme of P(VP-*co*-HEMA) hydrogels; **a** HEMA; **b** VP; **c** blocky sequence with DP = 50; **d** random sequence with DP = 50; **e** *N*,*N*′-methylenebisacrylamide (MBA); **f** configuration of the cross-linking point; **g** extended network with periodic boundary condition; **h** D-glucose; **i** ascorbic acid; equilibrated structure of the hydrogels with **j** D-glucose and with **k** ascorbic acid

*N*,*N*′-methylenebisacrylamide (MBA) (Fig. 1e) was used as the cross-linker to produce a three-dimensional network structure. To form a three-dimensional network structure as shown in Fig. 1f, we placed MBA at one end of each P(VP-*co*-HEMA) chain and then arranged all chains to participate in the network structure through periodic boundary conditions. It should be noticed that the topology of our current model is very ideal, having 6 chain-ends

connected without any structural variations such as free dangling ends and self-looping, which is deliberately chosen to remove the topological diversity in our modeling study as used in the previous studies [54, 55, 57, 58], while experimental systems have 2–4 chain-ends connected via one cross-linker with structural variations. We think that the current theoretical topology provides the same topological condition to both sequences to investigate the effect of monomeric sequence. Since such initial structure has non-physical strained conformation (Fig. 1g), we applied a molecular mechanics (energy minimization) and annealing procedure to relax the system to a physically meaningful structure as employed in our previous studies [54, 55, 57–62]. The annealing procedure accelerates the equilibration by driving the system repeatedly through sequential thermal (between 300 and 600 K) and pressure (between 50 and 110 % of the expected density) annealing cycles. This procedure helps the system quickly escape from various local minima and thereby efficiently reaches an equilibrated structure. Following the system construction, a canonical ensemble (NVT) and subsequent isothermal-isobaric ensemble (NPT) MD simulations were carried out to equilibrate the system for 200 ps and 16 ns, respectively, at 310.15 K. After equilibration, we used Monte Carlo techniques to add the guest molecules, D-glucose (Fig. 1h) or ascorbic acid (Fig. 1i), into the hydrogel systems. The distance between each guest molecule was controlled over 15 Å (which is the cutoff distance for van der Waals interaction) to avoid the interaction between the guest molecules at the beginning. Since glucose is mostly found in cyclic form and exists as pyranose in aqueous solution, we chose $\beta$-D-glucose for the guest molecule. We also chose L-ascorbic acid (vitamin C) in this study. Other variation in chemical structures such as degradation or oxidation form of guest molecules was not considered during the simulations. The positions of each guest molecule were randomly selected in the model systems. All of the systems were equilibrated by running 10–40 ns NPT MD simulations at 310.15 K. Data collection for the analysis was performed during a subsequent 10 ns NPT MD simulation.

Throughout this simulation, the hydrogel systems were described using the generic DREIDING force field [63] and F3C water force field [64]. These force fields have been successfully used for studies on various hydrated polymeric network systems such as polymer membranes [59–62, 65–67] and hydrogels [54, 55, 57, 58]. The total potential energy is given as follows:

$$E_{\text{total}} = E_{\text{vdW}} + E_{\text{Q}} + E_{\text{bond}} + E_{\text{angle}} + E_{\text{torsion}} + E_{\text{inversion}} \quad (2)$$

where $E_{\text{total}}$ denotes the total energy and $E_{\text{vdW}}$, $E_{\text{Q}}$, $E_{\text{bond}}$, $E_{\text{angle}}$, $E_{\text{torsion}}$, and $E_{\text{inversion}}$ are the energy components contributed from van der Waals, electrostatic, bond stretching, angle bending, torsion, and inversion components, respectively. All simulations were performed with the LAMMPS (Large-scale Atomic/Molecular Massively Parallel Simulator) code from Plimpton at Sandia National Laboratory [68, 69]. The equations of motion were integrated using a Verlet velocity algorithm [70] with a time step of 1.0 fs. A Nose–Hoover-type thermostat [71–73] was applied with a damping relaxation time of 0.1 ps. The individual atomic charges were assigned using the charge equilibration (QEq) method [74]. The atomic charges of the water molecules were assigned from the F3C water model. The particle–particle particle-mesh (PPPM) method [75] was used to calculate the long-range correction of electrostatic interactions.

## 3 Results and discussion

### 3.1 Equilibrated structure

Snapshots from the final MD simulations for the 80 wt. % water content cases are shown in Fig. 2 (other water content cases are not shown here due to their visual similarity), in which the differences in the monomeric sequences of the hydrogels are clearly observed. The random P(VP-*co*-HEMA) hydrogels contain more dispersed monomeric units (Fig. 2a, c), while the blocky P(VP-*co*-HEMA) hydrogels have a more segregated structure (Fig. 2b, d). Two independent hydrogel models for each monomer sequence were prepared that contained three molecules of either D-glucose or ascorbic acid, corresponding to a concentration of 0.03–0.14 M. The characteristics of the equilibrated P(VP-*co*-HEMA) hydrogels are shown in Table 1.

### 3.2 Distribution of guest molecules

To check the distribution of the guest molecules, we analyzed the pair correlation function (PCF) of the guest molecules with the P(VP-*co*-HEMA) hydrogels. The PCF, $g_{A-B}(r)$ is the probability density of finding atoms $A$ and $B$ at a distance $r$ averaged over the equilibrium trajectory as calculated by

$$g_{A-B}(r) = \left(\frac{n_B}{4\pi r^2 \mathrm{d}r}\right) \Big/ \left(\frac{N_B}{V}\right) \quad (3)$$

where $n_B$ is the number of $B$ particles located at a distance $r$ in a shell of thickness d$r$ from the $A$ particle, $N_B$ is the number of $B$ particles in the system, and $V$ is the total volume of the system. Using this function, it is possible to determine in what environment the guest molecules are found. For this study, $\rho g(r)$, the product of $g(r)$ and the number density ($\rho$), is used instead of $g(r)$ to directly

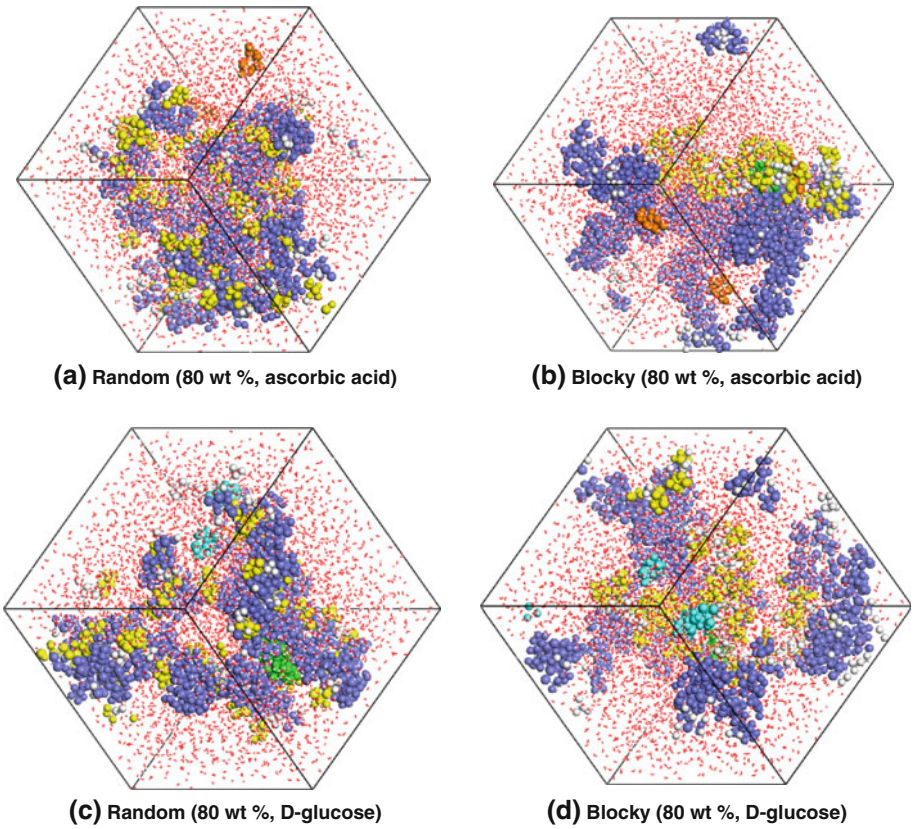


**Fig. 2** Equilibrated *random* P(VP-*co*-HEMA) hydrogels with 80 wt. % water content. **a** and **b** for ascorbic acids in the random sequence hydrogel and the blocky sequence hydrogel, respectively; **c** and **d** for D-glucose in the random sequence hydrogel and the blocky sequence hydrogel, respectively. *Blue*, *yellow*, *green*, *orange*, and *cyan colors* denote VP, HEMA, MBA, ascorbic acid, and D-glucose, respectively. The oxygens of the water molecules are represented by *red colors* with a smaller ball size for a clear view

compare the absolute values between various systems. For quantitative analysis, the coordination number (CN) is calculated by integrating the first peak in the PCF. Figure 3 shows the three pairs of interest: (i) $\rho g_{\mathrm{N(VP)-}O\mathrm{(guest\,molecule)}}$ for the nitrogen of the VP (N (VP)) and the oxygen of the guest molecule (O (guest molecule)); (ii) $\rho g_{\mathrm{C(HEMA)-O(guest\,molecule)}}$ for the alpha carbon of the HEMA (C (HEMA)) and O (guest molecule); and (iii) $\rho g_{\mathrm{O(HEMA)-O(guest\,molecule)}}$ for the oxygen of the hydroxyl group of the HEMA (O (HEMA)) and O (guest molecule).

In Figs. 4 and 5, the $\rho g(r)$ values of the P(VP-*co*-HEMA) hydrogels with the random and blocky sequence with 20, 40, and 80 wt. % water content are shown. These figures show that the $\rho g_{\mathrm{O(HEMA)-O(guest\,molecule)}}$ values are nonzero for distance of approximately $r > 2.5$ Å, while the other $\rho g(r)$s appear for $r > 3.5$ Å. This is because the location of O (HEMA) (the oxygen of the terminal hydroxyl group in HEMA) unit is more accessible for the guest molecules in comparison with C (HEMA) and N (VP).

By comparing Fig. 4a, b for 20 wt. % water content, we found that the peak intensities for the $\rho g_{\mathrm{C(HEMA)-O(ascorbic\,acid)}}$ and the $\rho g_{\mathrm{O(HEMA)-O(ascorbic\,acid)}}$ depend on the monomer sequence of P(VP-*co*-HEMA), with $\rho g_{\mathrm{X(HEMA)-O(ascorbic\,acid)}}$ (X=C or O) possessing a smaller intensity at $\sim 5$ Å for the blocky sequence hydrogel. As shown in Table 2, the calculated coordination numbers (CNs) for 20 wt. % water content obtained from the first peak of $\rho g_{\mathrm{C(HEMA)-O(ascorbic\,acid)}}$ and $\rho g_{\mathrm{O(HEMA)-O(ascorbic\,acid)}}$ for the blocky sequence are 2–4.3 times smaller than those for the random sequence. The PCFs for D-glucose (Fig. 5a, b) also show dependency on the monomer sequence, with the CN results for 20 wt. % water content (Table 2), showing that the CNs from the $\rho g_{\mathrm{C(HEMA)-O(D-glucose)}}$ and the $\rho g_{\mathrm{O(HEMA)-O(D-glucose)}}$ for the blocky sequence show smaller values than do those for the random sequence. On the other hand, the intensity of the first peak for $\rho g_{\mathrm{N(VP)-O(ascorbic\,acid)}}$ and $\rho g_{\mathrm{N(VP)-O(D-glucose)}}$ is less affected by the monomer sequence of the hydrogel than are those of $\rho g_{\mathrm{X(HEMA)-O(guest\,molecule)}}$, as shown in Figs. 4 and 5. However, the CNs from the blocky sequence show higher values than those from the random sequence, as shown in Table 2. The CNs from $\rho g_{\mathrm{N(VP)-O(ascorbic\,acid)}}$ and $\rho g_{\mathrm{N(VP)-O(D-glucose)}}$ show larger values than those of $\rho g_{\mathrm{X(HEMA)-O(ascorbic\,acid)}}$ and $\rho g_{\mathrm{X(HEMA)-O(D-glucose)}}$ for both monomeric sequences, indicating that the guest molecule has a greater accessibility to the VP units than the HEMA units in both monomeric sequences. We expect that hydrophilic guest molecules, such as ascorbic acid and D-glucose, may tend to be more associated with the VP units because the VP units are more hydrophilic than the HEMA units, as evaluated by previous experiments [26, 28, 34, 76, 77] and simulations [54, 55]. The guest molecules can be confined within the polymer network in low hydration conditions, as distinctly

**Table 1** Characteristics of the hydrogels

| Monomeric sequence | Random | | | | | | Blocky | | | | | |
|---|---|---|---|---|---|---|---|---|---|---|---|---|
| Monomer composition | VP/HEMA = 37: 13 | | | | | | VP/HEMA = 37: 13 | | | | | |
| Degree of randomness | 1.17 | | | | | | 0.10 | | | | | |
| Cross-linking molecular weight, $M_c$ | 5,804.16 | | | | | | 5,804.16 | | | | | |
| Simulated temperature (K) | 310.15 | | | | | | 310.15 | | | | | |
| Guest molecule | Ascorbic acid | | | D-glucose | | | Ascorbic acid | | | D-glucose | | |
| Water content | 20 wt. % | 40 wt. % | 80 wt. % | 20 wt. % | 40 wt. % | 80 wt. % | 20 wt. % | 40 wt. % | 80 wt. % | 20 wt. % | 40 wt. % | 80 wt. % |
| Number of water molecule | 248 | 661 | 3,969 | 248 | 661 | 3,969 | 248 | 661 | 3,969 | 248 | 661 | 3,969 |
| Number of guest molecules (concentration, M) | 3 (0.14) | 3 (0.10) | 3 (0.03) | 3 (0.14) | 3 (0.10) | 3 (0.03) | 3 (0.14) | 3 (0.10) | 3 (0.03) | 3 (0.14) | 3 (0.10) | 3 (0.03) |
| Density (g/cm$^3$) | 1.065 ± 0.007 | 1.034 ± 0.007 | 1.016 ± 0.004 | 1.058 ± 0.007 | 1.035 ± 0.007 | 1.016 ± 0.003 | 1.062 ± 0.007 | 1.032 ± 0.006 | 1.014 ± 0.004 | 1.046 ± 0.007 | 1.031 ± 0.007 | 1.014 ± 0.004 |
| Simulated volume (Å$^3$) | 35,669 ± 226 | 48,664 ± 329 | 146,984 ± 518 | 35,904 ± 226 | 48,631 ± 326 | 147,025 ± 504 | 35,749 ± 221 | 48,781 ± 307 | 147,205 ± 508 | 36,313 ± 243 | 48,832 ± 339 | 147,210 ± 514 |
| Mesh size, $\xi$ (Å) | 32.92 ± 0.07 | 36.51 ± 0.08 | 52.77 ± 0.06 | 32.99 ± 0.07 | 36.50 ± 0.08 | 52.78 ± 0.06 | 32.94 ± 0.07 | 36.54 ± 0.08 | 52.80 ± 0.06 | 33.11 ± 0.07 | 36.55 ± 0.08 | 52.80 ± 0.06 |

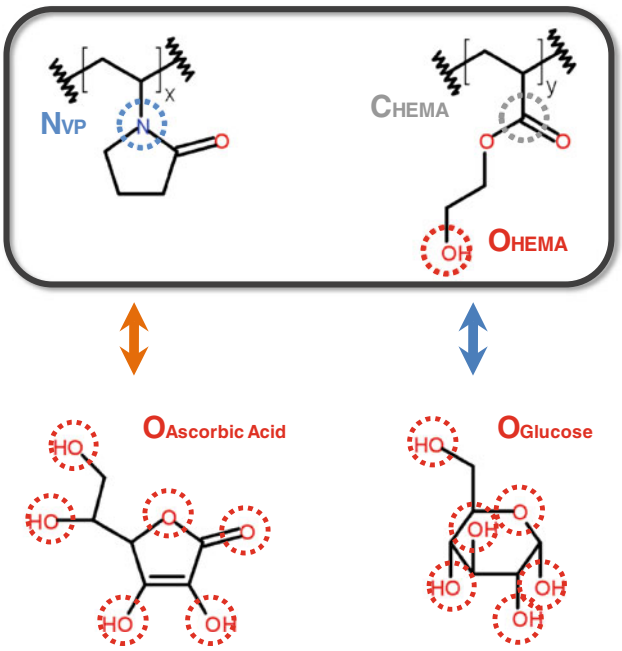


**Fig. 3** Atoms used to calculate the pair correlation function

shown for a water content of 20 wt. %. This confinement can lead to the guest molecules having more interactions with the polymer network, especially with the more hydrophilic VP segments. Detailed discussions of the confinement are given in next section.

To explain this monomeric sequence effect on P(VP-*co*-HEMA) hydrogel with 20 wt. % water content, we calculated the solvent-accessible surface area (SASA) of the monomeric units to check the accessible surface for the guest molecule. The probe radius for calculating the SASA was set to be 2.78 and 2.71 Å, which are the hydrodynamic radii ($r_h$) of D-glucose and ascorbic acid, respectively [57]. As shown in Table 3, the SASA of the VP unit has a larger accessible area than the HEMA unit for the guest molecules, which agrees with the results of the PCFs and CNs. It is also observed that comparing monomer sequences, the blocky sequence hydrogel has accessible areas for the VP units and the HEMA units that are 29–37 % and 4–15 % larger than those of the random sequence hydrogel, respectively. The SASA of the VP units is more sensitive to the effects of the monomeric sequence than the SASA of the HEMA units. We think this is due to the random distribution of the HEMA units among the VP units in the random sequence hydrogel. In this case, the HEMA units can screen out the access of the probe toward the VP units in the random sequence. As we mentioned above, the O (HEMA) unit is more accessible for the probe, especially in the random sequence, and the HEMA unit is longer than the VP unit by ~36 % (the root-mean-square radius of gyration is $1.92 \pm 0.33$ Å for the VP unit and $2.61 \pm 0.01$ Å for the HEMA unit at 310 K). Therefore, the guest molecules can be excluded from the VP units by the HEMA units in the random sequence, which leads to smaller CNs for $\rho g_{N(VP)-O(\text{guest molecule})}$ and higher CNs for $\rho g_{X(HEMA)-O(\text{guest molecule})}$ in the random sequence than in the blocky sequence at the low water content.

However, this monomeric sequence effect is significantly reduced with 40 wt. % water content (see Figs. 4c, d, 5c, d) and disappears completely with 80 wt. % water content (see Figs. 4e, f, 5e, f). This occurs because the polymer chains are swollen with increasing water content. Therefore, the hydrophilic guest molecules, such as ascorbic acid [78] and D-glucose [79], are more likely to be associated with water molecules than with the polymer network at these high water contents. To determine in what environment the guest molecules are associated with the water molecules, we characterized the water distribution around the guest molecules by PCF using the oxygen of the guest molecule and the oxygen of the water molecule ($\rho g_{O(\text{guest molecules})-O(\text{water})}$), as shown in Fig. 6. The analysis of the water CN for the guest molecules is given in Table 4. It is clearly shown that the intensities of the PCFs and CNs are increased with increasing water content, meaning that the interaction between the guest molecules and the P(VP-*co*-HEMA) is screened by water molecules.

### 3.3 Diffusion of guest molecules

The diffusion of guest molecules is another interesting aspect of hydrogels because of its importance to bio-applications, such as tissue engineering and drug delivery, in which small guest molecules can be transported. From numerous studies focusing on the variables affecting solute transport [80–84], it is understood that the transport properties are strongly dependent upon many factors, such as mesh size, swelling ratio, ionization, ionic strength, pH condition, and temperature. In our simulations, the number of guest molecules in all P(VP-*co*-HEMA) hydrogels was the same to check the effect of the water content on the transport properties of the guest molecule. The mean square displacement (MSD) of the guest molecules in the hydrogels was obtained from the last 5 ns of our NPT MD simulations to calculate the diffusion coefficients (D), as defined by

$$D = \lim_{t\to\infty} \frac{1}{6t} \left\langle (r(t) - r(0))^2 \right\rangle \tag{4}$$

where $r(t)$ and $r(0)$ are the positions of the target molecules at a time $t$ that is greater than 0 and at $t = 0$, respectively. The MSD follows a power law in time with exponent ($\alpha$) that

$$\left\langle (r(t) - r(0))^2 \right\rangle \sim t^{\alpha} \tag{5}$$

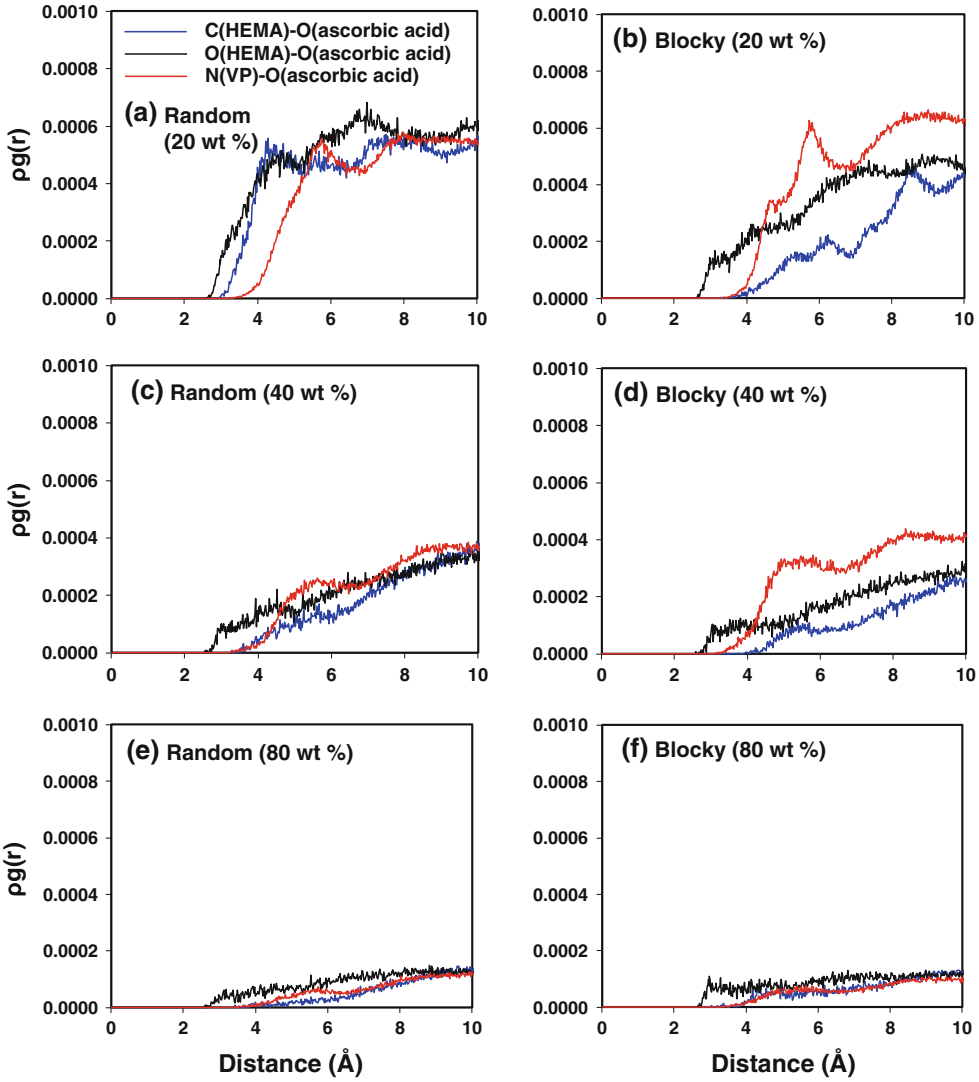


**Fig. 4** Pair correlation functions of ascorbic acid in the P(VP-*co*-HEMA) hydrogel: ascorbic acid in the random sequence with 20 wt. % (**a**), 40 wt. % (**c**), and 80 wt. % water content (**e**) and in the blocky sequence with 20 wt. % (**b**), 40 wt. % (**d**), and 80 wt. % water content (**f**)

The diffusion is normal if MSD, $\left\langle (r(t) - r(0))^2 \right\rangle$, is proportional to time $t$ with $\alpha = 1$. If the diffusion of molecules is hindered or obstructed by the structure of the system, the value of $\alpha$ is smaller than 1, which is known as an anomalous subdiffusion [85, 86]. This has been observed in various systems, such as membranes [87, 88], hydrogels [89], and porous media [90]. Previously, Jang et al. [57] reported that the ascorbic acid and D-glucose in the poly(ethylene oxide)–poly(acrylic acid) double-network hydrogel with 76 % water content showed values of $\alpha$ between 0.74 and 0.82.

In this study (see Fig. 7), we obtained $\alpha$ values of 0.36–0.47 for 20 wt. % water content, 0.62–0.80 for 40 wt. % water content, and 0.79–0.89 for 80 wt. % water content P(VP-*co*-HEMA) hydrogels, respectively. These results clearly indicate that the diffusion of the guest molecules in low hydration hydrogel systems (20 wt. % water content) corresponds to the anomalous subdiffusion and is seriously depressed and this anomalous subdiffusion approaches normal diffusion as the water content increases to a high level of hydration.

The diffusion coefficients for ascorbic acid and D-glucose for each monomer sequence hydrogel are summarized in Table 5. Unfortunately, there are no available experimental diffusion coefficients for our particular systems to make a direct comparison with these calculated results. However, we found several experimental diffusion coefficient data for the guest molecule in bulk water at room temperature. Thus, we also simulated reference systems containing the guest molecules in a bulk water phase to calculate the diffusion coefficient for comparison with the experimental one, which validates our simulations. Our reference systems were built to contain 1,200 water molecules and three guest molecules and equilibrated by running 10 ns NPT MD simulations at 298.15 K. Then, a subsequent 10 ns NPT MD simulation was performed for

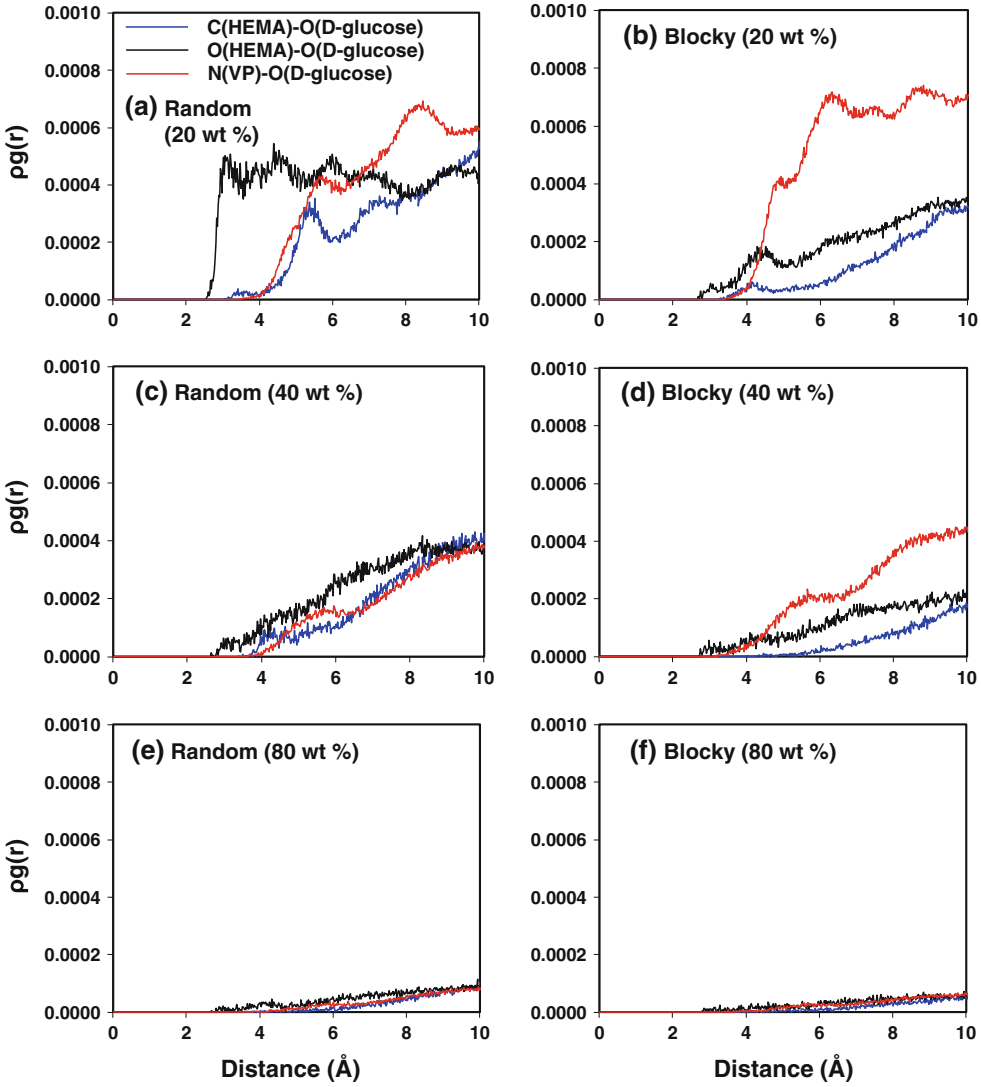


**Fig. 5** Pair correlation functions of D-glucose in P(VP-*co*-HEMA) hydrogel: ascorbic acid in the random sequence with 20 wt. % (**a**), 40 wt. % (**c**), and 80 wt. % water content (**e**) and in the blocky sequence with 20 wt. % (**b**), 40 wt. % (**d**), and 80 wt. % water content (**f**)

**Table 2** Guest molecule coordination number (CN) from the X–O (guest molecule) pair in the P(VP-*co*-HEMA) hydrogel

| Guest molecule | X | CN | | | Range of pair correlation distance, $r$ (Å) |
|---|---|---|---|---|---|
| | | 20 wt. % | 40 wt. % | 80 wt. % | |
| Ascorbic acid | $C_{HEMA}$ (random) | 0.17 ± 0.02 | 0.03 ± 0.00 | 0.00 ± 0.01 | <5.1 |
| | $O_{HEMA}$ (random) | 0.18 ± 0.02 | 0.06 ± 0.02 | 0.03 ± 0.02 | <5.1 |
| | $N_{VP}$ (random) | 0.43 ± 0.03 | 0.22 ± 0.03 | 0.05 ± 0.03 | <6.8 |
| | $C_{HEMA}$ (blocky) | 0.04 ± 0.01 | 0.02 ± 0.02 | 0.02 ± 0.03 | <5.5 |
| | $O_{HEMA}$ (blocky) | 0.09 ± 0.01 | 0.04 ± 0.01 | 0.03 ± 0.03 | <5.1 |
| | $N_{VP}$ (blocky) | 0.45 ± 0.01 | 0.30 ± 0.02 | 0.06 ± 0.04 | <6.8 |
| D-glucose | $C_{HEMA}$ (random) | 0.10 ± 0.01 | 0.05 ± 0.02 | 0.00 ± 0.00 | <5.8 |
| | $O_{HEMA}$ (random) | 0.20 ± 0.03 | 0.05 ± 0.01 | 0.01 ± 0.01 | <5.1 |
| | $N_{VP}$ (random) | 0.35 ± 0.02 | 0.14 ± 0.02 | 0.02 ± 0.00 | <6.8 |
| | $C_{HEMA}$ (blocky) | 0.01 ± 0.01 | 0.00 ± 0.00 | 0.00 ± 0.00 | <4.7 |
| | $O_{HEMA}$ (blocky) | 0.05 ± 0.02 | 0.02 ± 0.01 | 0.01 ± 0.01 | <5.1 |
| | $N_{VP}$ (blocky) | 0.55 ± 0.01 | 0.19 ± 0.02 | 0.02 ± 0.01 | <6.8 |

**Table 3** Solvent-accessible surface area of VP units and HEMA units with respect to guest molecules

| | Random sequence | | Blocky sequence | |
|---|---|---|---|---|
| | VP (Å$^2$) | HEMA (Å$^2$) | VP (Å$^2$) | HEMA (Å$^2$) |
| Ascorbic acid (probe radius = 2.71 Å) | 1,465 ± 75 | 653 ± 66 | 1,893 ± 88 | 678 ± 20 |
| D-glucose (probe radius = 2.78 Å) | 1,650 ± 109 | 690 ± 56 | 2,253 ± 66 | 796 ± 51 |

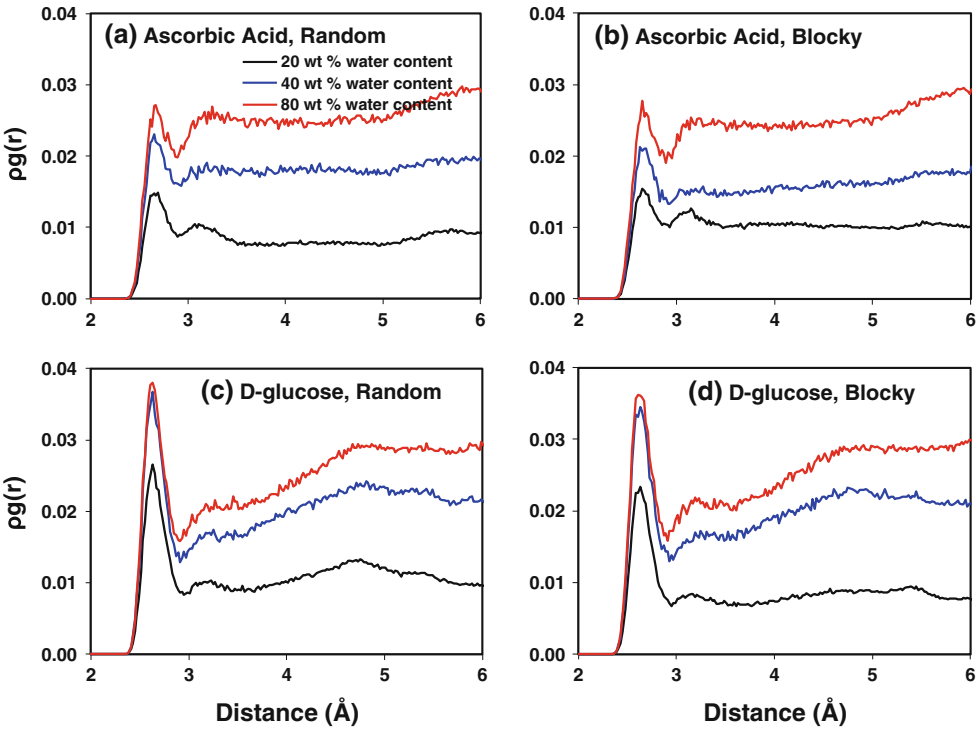


**Fig. 6** Pair correlation functions of O(ascorbic acid)–O(water) in random sequence (**a**) and in blocky sequence (**b**); pair correlation functions of O(D-glucose)–O(water) in random sequence (**c**) and in blocky sequence (**d**)

**Table 4** Coordination number (CN) from the O(guest molecule)–O(water) pair in a P(VP-*co*-HEMA) hydrogel

| | Random sequence | Blocky sequence | Range of pair correlation distance, $r$ (Å) |
|---|---|---|---|
| Ascorbic acids | | | |
| 20 wt. % | 0.45 ± 0.02 | 0.48 ± 0.02 | <2.9 |
| 40 wt. % | 0.72 ± 0.03 | 0.66 ± 0.03 | <2.9 |
| 80 wt. % | 0.87 ± 0.02 | 0.85 ± 0.01 | <2.9 |
| D-glucoses | | | |
| 20 wt. % | 0.69 ± 0.04 | 0.62 ± 0.02 | <2.9 |
| 40 wt. % | 0.97 ± 0.02 | 0.96 ± 0.01 | <2.9 |
| 80 wt. % | 1.05 ± 0.01 | 1.05 ± 0.01 | <2.9 |

data collection. The diffusion coefficients were determined to be 5.76 × $10^{-6}$ cm$^2$/s ($\alpha = 1$) and 6.62 × $10^{-6}$ cm$^2$/s ($\alpha = 1$) for ascorbic acid and D-glucose, respectively, which are in a good agreement with the experimental values of 5.80–5.97 × $10^{-6}$ cm$^2$/s and 6.51–6.78 × $10^{-6}$ cm$^2$/s for ascorbic acid [91] and D-glucose [92–94], respectively. We also found the diffusion coefficient of ascorbic acid and D-glucose in the PEO hydrogel system with 76 % and 80 wt. % water content, which are comparable with the 80 % water content of P(VP-*co*-HEMA) hydrogel system in this study. Jang et al. [57] reported that the diffusion coefficient of ascorbic acid and D-glucose in the poly(ethylene oxide)–poly(acrylic acid) double-network hydrogel with 76 % water content is 1.11–2.53 × $10^{-6}$ cm$^2$/s and 1.07–2.49 × $10^{-6}$ cm$^2$/s at 300 K from their simulation study, respectively. Myung et al. [95] experimentally observed that the diffusion coefficient of glucose is 0.9–1.8 × $10^{-6}$ cm$^2$/s in poly(ethylene glycol) hydrogels with 80 wt. % water content at room temperature.

Table 5 shows that the diffusion coefficients of ascorbic acid and D-glucose in the random sequence hydrogel are twice as high as in the blocky sequence hydrogel for 20 wt. % content, while the difference is decreased by ~18 and ~8 % when increasing the water content to 40 wt. % and 80 wt. %, respectively. At the low water content, the guest molecule has more interactions with the *block* of VP units

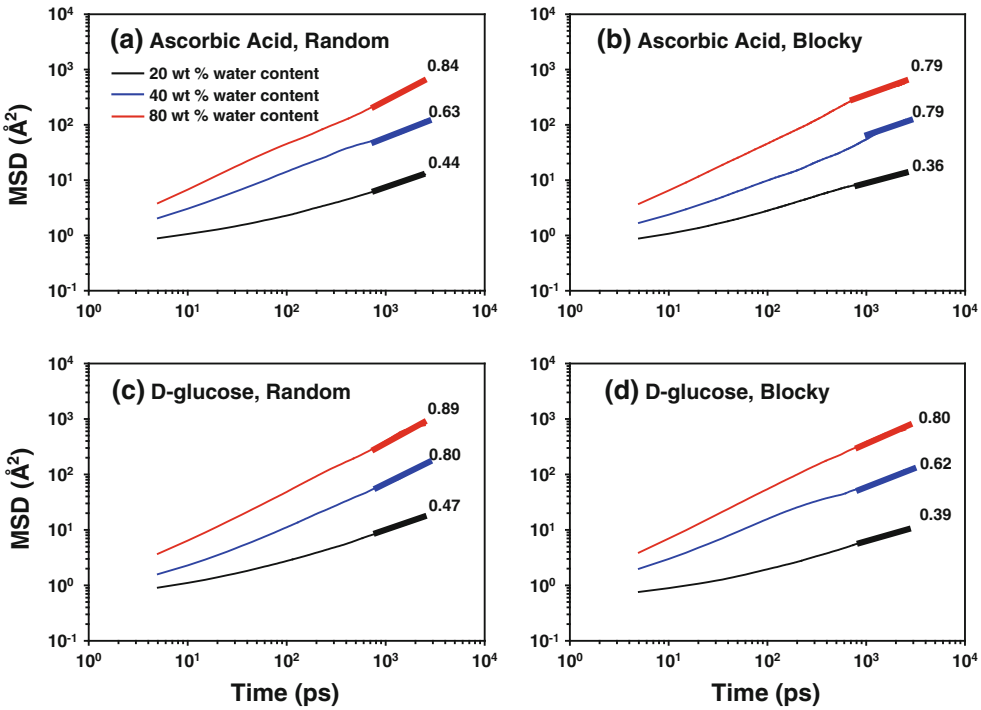


**Fig. 7** Mean square displacement (MSD) of logarithmic plots for the guest molecules in the P(VP-*co*-HEMA) hydrogel, with ascorbic acid in a random sequence (**a**) and blocky sequence (**b**) and with D-glucose in a random sequence (**c**) and blocky sequence (**d**)

**Table 5** Chemical formula, molecular weight, and diffusion coefficient of guest molecules at 310 K

| | Ascorbic acid | | D-glucose | |
|---|---|---|---|---|
| Chemical formula | $C_6H_8O_6$ | | $C_6H_{12}O_6$ | |
| Molecular weight, MW | 176.126 | | 180.157 | |
| Monomeric sequence | Random | Blocky | Random | Blocky |
| Diffusion coefficient, $D$ ($\times 10^{-6}$ cm$^2$/s) | | | | |
| 20 wt. % water content | 0.02 ± 0.00 | 0.01 ± 0.00 | 0.02 ± 0.00 | 0.01 ± 0.00 |
| 40 wt. % water content | 0.80 ± 0.02 | 0.68 ± 0.03 | 0.79 ± 0.01 | 0.67 ± 0.01 |
| 80 wt. % water content | 2.85 ± 0.06 | 2.83 ± 0.04 | 2.72 ± 0.06 | 2.51 ± 0.05 |
| 100 wt. % water content (bulk water)[a] | 5.76 ± 0.02 | | 6.62 ± 0.02 | |

[a] The simulation with 100 wt. % water content was performed using a bulk water system consisting of 1,200 water molecules

in the blocky sequence hydrogel than in the random sequence hydrogel. This leads to reduced diffusion of the hydrophilic guest molecules in the blocky sequence hydrogel, a result which is consistent with the analyses of the PCFs and CNs. Considering that even water molecules diffuse less when near a hydrophilic substrate in the highly confined environment [96, 97], therefore, it seems that a hydrophilic domain such as the VP units in the blocky sequence hydrogel can suppress the diffusivity of the hydrophilic molecules at the low water content. However, the monomeric sequence effect on the diffusion coefficients of the guest molecule is significantly decreased with an increasing water content.

In order to characterize the diffusion mechanism of the guest molecules, we monitored the total displacement of the center of mass of the guest molecules from the initial position to their position at time $t$ during the last 10 ns of the NPT MD simulation (see Fig. 8). It is observed that the total displacement of the guest molecules is significantly suppressed at the low water content (20 wt. % water content). The guest molecules at 20 wt. % water content seem to be bound at a certain location within the hydrogel or diffused within a confined pocket within the hydrogel. It is observed that the guest molecules in the 40 wt. % and the 80 wt. % water content hydrogels can diffuse through a water channel in the polymer network.

The diffusion of small guest molecules in the polymer network also depends on the geometrical conditions such as the size and distribution of the pores in addition to the molecular interactions. Thus, we analyzed the porosity of the hydrogels to investigate the effect of geometry on the diffusion of guest molecules by comparison with theoretical models. First, a simple cubic void (10 Å × 10 Å × 10 Å, Fig. 9c) was built in a periodic box (30 Å × 30 Å × 30 Å,

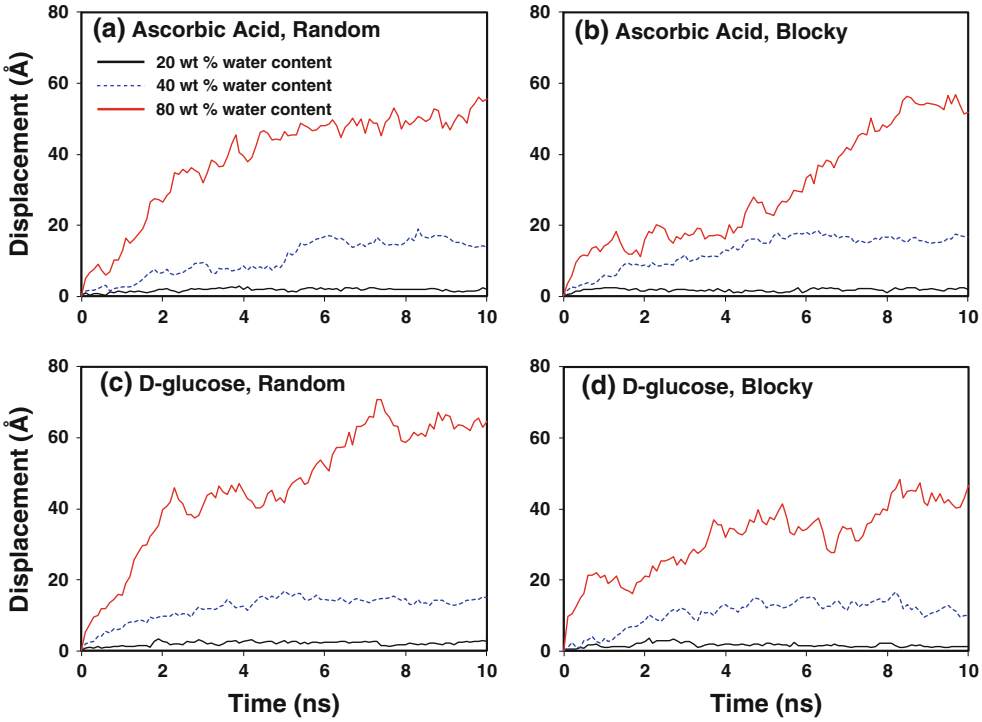


**Fig. 8** Total displacement of the center of mass of the guest molecules in the P(VP-*co*-HEMA) hydrogel during the last 10 ns of the NPT MD simulation for ascorbic acid in the random sequence (**a**) and in the blocky sequence (**b**) and for D-glucose in the random sequence (**c**) and in the blocky sequence (**d**)

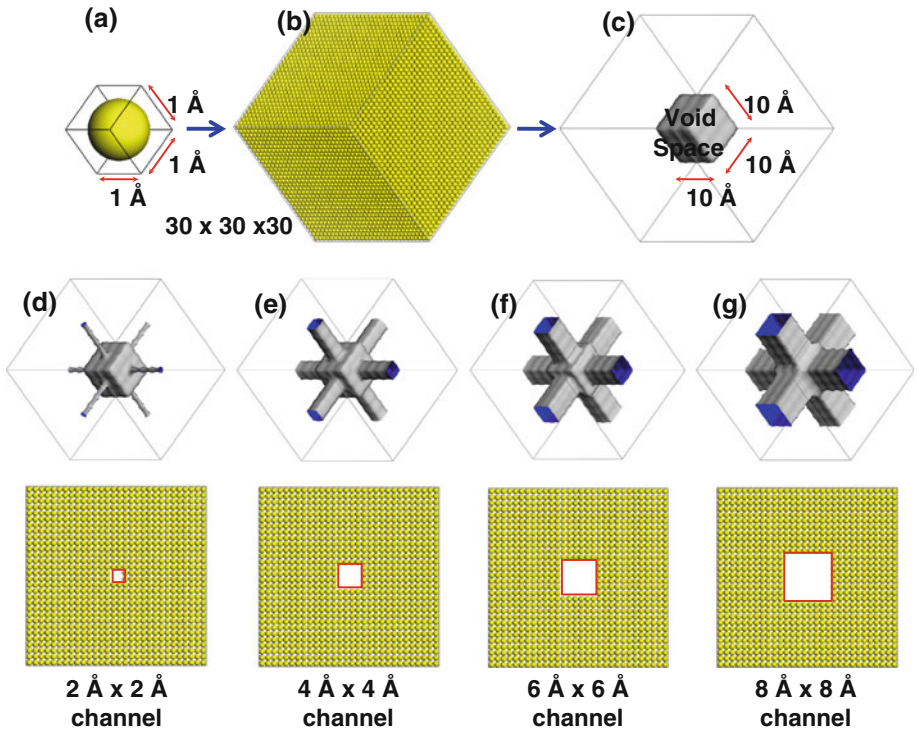


**Fig. 9** Theoretical models to investigate the relationship between the size of the channel in the system and the available surface area; **a** a unit structure with a dummy atom with a van der Waals radius of 0.5 Å; **b** a superstructure made of 30 × 30 × 30 unit structures; and **c** a model with a cubical void of 10 × 10 × 10 Å at the center. Models with various cross-sectional areas for the channel: **d** 2 Å× 2 Å; **e** 4 Å × 4 Å; **f** 6 Å × 6 Å; and **g** 8 Å × 8 Å. The dummy atoms are invisible in models **c**, **d**, **e**, **f,** and **g** to allow for a clear view of the void and the channels

Fig. 9b) using a dummy atom with a van der Waals radius of 0.5 Å (Fig. 9a). Then, the simple cubic void was connected via channels of four different cross-sectional areas: 2 × 2 Å (Fig. 9d), 4 × 4 Å (Fig. 9e), 6 × 6 Å (Fig. 9f), and 8 × 8 Å (Fig. 9g). If the spherical molecule has a sufficiently small radius, then it can diffuse through the channel. Otherwise, the guest molecule is confined within the simple cubic void. Using such a theoretical model (Fig. 9) with the solvent-accessible surface analysis, we evaluated the inner-surface area of the theoretical model, which depends on the probe radius. As shown in Fig. 10, the inner-surface area decreases with an increasing probe radius because it is

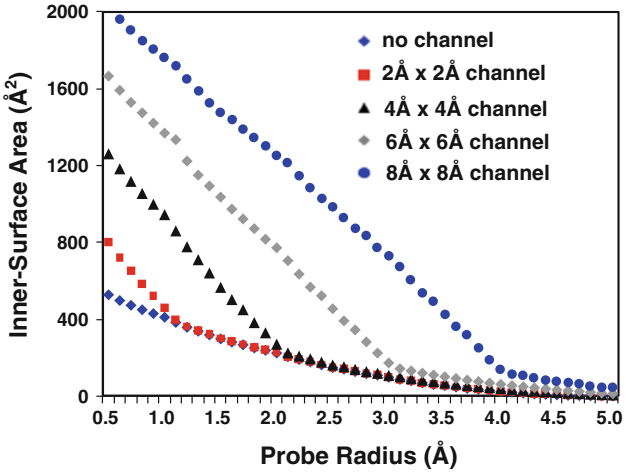


**Fig. 10** Change in the inner-surface area from the theoretical models (Fig. 9) as a function of probe radius

actually the contacting surface area for a given probe radius. Thus, if the probe radius is larger than the radius of the channel size, the inner-surface of the channel is not counted in the measurement.

From Fig. 10, the threshold value of the probe radius to detect the channel in models in Fig. 9d–g is clearly observed at 1, 2, 3, and 4 Å, respectively, which exactly matched the size of the radius of the channel. In other words, a solute can diffuse through the channel to move toward other sites if the solute radius size is smaller than the threshold value for the model. Otherwise, a solute can be confined within the pore (cubic void). Thus, we believe that this analysis can discriminate the difference in porosity between the hydrogels on nanometer-scale.

Figure 11 shows that the change of the inner-surface area of the hydrogels depends on the water content. We did not see a clear threshold of the probe radius, but rather observed the intermediate zone between two linear regimes (see the inset of Fig. 11a), due to the complicated structures of the hydrogels with various sizes and shapes of channels and cages. If a solute has a radius within the range of the intermediate zone, then it can diffuse through the proper channel, but it can also be confined simultaneously by smaller channels. Because the hydrodynamic radii of the ascorbic acid and D-glucose are 2.71 and 2.78 Å, respectively, it is expected that they are confined within the local voids in the hydrogel for a 20 wt. % water content hydrogel. The hydrodynamic radius of the guest molecule is within the range of the intermediate zone at 40 wt. % water content, and therefore, the guest diffusion is restricted within the hydrogel. At 80 wt. % water content, the threshold of the probe radius is not observed at all if the range of the probe radius is less than 5 Å, indicating that the guest molecule can diffuse through the hydrogel easily. These results are consistent with their diffusion behavior discussed above (see Figs. 7, 8; Table 5). Thus, the diffusion of the guest molecules is increased with increasing water content up to the maximum value observed in the bulk water phase (Table 5).

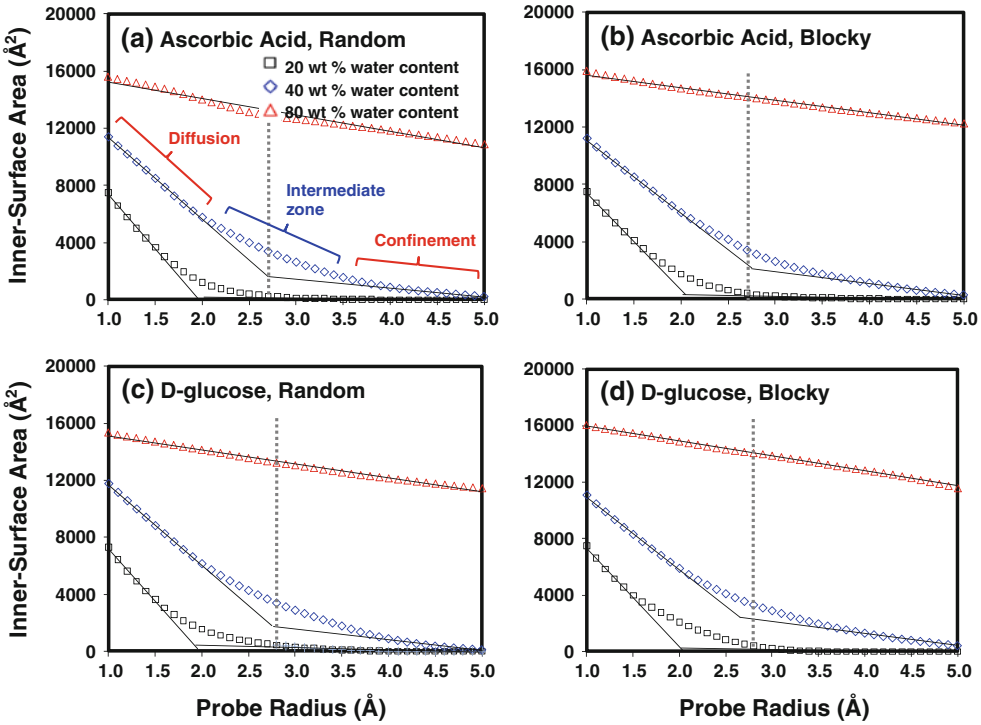


**Fig. 11** Change in the inner-surface area from the simulated hydrogels as a function of the probe radius; ascorbic acid in the random sequence (**a**) and in the blocky sequence (**b**) and D-glucose in the random sequence (**c**) and in the blocky sequence (d). The *dot-line* indicates the radius of either ascorbic acid or D-glucose. The *gray dot-line* indicates the hydrodynamic radius of the guest molecule

## 4 Conclusion

Using a full-atomistic MD simulation approach, we investigated P(VP-*co*-HEMA) hydrogels containing 20, 40, and 80 wt. % water at 310.15 K with both random and blocky sequences. Ascorbic acid and D-glucose were used to study the effect of the monomeric sequence on the diffusion of small guest molecules within the hydrogels. By analyzing the pair correlation functions, it was found that the guest molecule has greater accessibility to the VP units than to the HEMA units with both monomeric sequences due to its higher hydrophilicity compared to the HEMA units. The monomeric sequence effect on the P(VP-*co*-HEMA) hydrogel is most obvious at 20 wt. % water content, whereas this monomeric sequence effect is significantly reduced with 40 wt. % water content and disappears with 80 wt. % water content. This is because the hydrophilic guest molecules are more likely to be solvated with water molecules than with the polymer network at the high water content. Here, it should be noted that this water content dependency of the transport properties should also be affected by the other variables such as the degree of polymerization (DP) for the polymer chain. For example, if we use the DP of 30, which is smaller than the current DP value (50), we would see the effect of the monomeric sequence at higher water contents such as 40 or 60 wt. %. Since we determined the current DP in this study to set a common condition for both random and blocky sequences, it is appropriate to focus on the overall behavior of the hydrogel as a function of water content, rather than to see a specific water content. By analyzing the mean square displacement, the displacement of the guest molecules, and the inner-surface area, it is also found that guest molecules are confined in the system at 20 wt. % water content, resulting in highly anomalous subdiffusion. Therefore, the diffusion of the guest molecules is directly affected by their interaction with the monomer units, the monomeric sequence, and the geometrical confinement in the hydrogel at low water content, but the monomeric sequence effect and the restriction on the diffusion of the guest molecule are significantly decreased with increasing water content. This is mainly due to the increase in channel size in the hydrogels as revealed by the inner-surface area of the hydrogel. Therefore, in conclusion, the diffusion of guest molecules in hydrogels can be controlled by the monomeric sequence of the polymers at low water content conditions.

## References


1. Lowman AM, Peppas NA (1999) Hydrogels. Encyclopedia of controlled drug delivery, vol 2. Wiley, New York
2. Wichterle O, Lim D (1960) Hydrophilic gels for biological use. Nature 185(4706):117–118
3. Peppas NA (1997) Hydrogels and drug delivery. Curr Opin Colloid Interface Sci 2(5):531–537
4. Lee KY, Mooney DJ (2001) Hydrogels for tissue engineering. Chem Rev 101(7):1869–1879. doi:10.1021/Cr000108x
5. Tanaka Y, Gong JP, Osada Y (2005) Novel hydrogels with excellent mechanical performance. Prog Polym Sci 30(1):1–9
6. Peppas NA, Huang Y, Torres-Lugo M, Ward JH, Zhang J (2000) Physicochemical, foundations and structural design of hydrogels in medicine and biology. Annu Rev Biomed Eng 2:9–29
7. Ratner BD, Hoffman AS, Schoen FJ, Lemons JE (2004) Biomaterials science: an introduction to materials in medicine. Elsevier Academic Press, San Diego, CA
8. Montheard JP, Chatzopoulos M, Chappard D (1992) 2-Hydroxyethyl methacrylate (Hema)—chemical-properties and applications in biomedical fields. J Macromol Sci, Rev Macromol Chem Phys C32(1):1–34
9. Hoffman AS (2002) Hydrogels for biomedical applications. Adv Drug Deliv Rev 54(1):3–12
10. Peppas NA, Moynihan HJ, Lucht LM (1985) The structure of highly crosslinked poly(2-hydroxyethyl methacrylate) hydrogels. J Biomed Mater Res 19(4):397–411
11. Gokce M, Akata RF, KiremitciGumusderelioglu M (1996) 5-FU loaded pHEMA drainage implants for glaucoma-filtering surgery: device design and in vitro release kinetics. Biomaterials 17(9):941–949
12. KiremitciGumusderelioglu M, Gokce M, Akata RF (1996) A novel MMC-loaded pHEMA drainage device for the treatment of glaucoma: in vitro and in vivo studies. J Biomater Sci Polym Ed 7(10):857–869
13. Lu SX, Anseth KS (1999) Photopolymerization of multilaminated poly(HEMA) hydrogels for controlled release. J Control Release 57(3):291–300
14. Teijon JM, Trigo RM, Garcia O, Blanco MD (1997) Cytarabine trapping in poly(2-hydroxyethyl methacrylate) hydrogels: drug delivery studies. Biomaterials 18(5):383–388
15. Hsiue GH, Guu JA, Cheng CC (2001) Poly(2-hydroxyethyl methacrylate) film as a drug delivery system for pilocarpine. Biomaterials 22(13):1763–1769
16. Young CD, Wu JR, Tsou TL (1998) Fabrication and characteristics of polyHEMA artificial skin with improved tensile properties. J Membr Sci 146(1):83–93
17. Young CD, Wu JR, Tsou TL (1998) High-strength, ultra-thin and fiber-reinforced pHEMA artificial skin. Biomaterials 19(19): 1745–1752
18. Husain MT, Akhtar M, Akhtar N (1983) Report on evaluation of hydron film as burn wound dressing. Burns Incl Therm Inj 9(5):330–334
19. Nathan P, Robb EC, Law EJ, MacMillan BG (1982) A clinical study of antimicrobial agents delivered to burn wounds from a drug-loaded synthetic dressing. J Trauma 22(12):1015–1018
20. Lee SD, Hsiue GH, Kao CY, Chang PCT (1996) Artificial cornea: surface modification of silicone rubber membrane by graft polymerization of pHEMA via glow discharge. Biomaterials 17(6):587–595
21. Kidane A, Szabocsik JM, Park K (1998) Accelerated study on lysozyme deposition on poly(HEMA) contact lenses. Biomaterials 19(22):2051–2055
22. Arica MY, Senel S, Alaeddinoglu NG, Patir S, Denizli A (2000) Invertase immobilized on spacer-arm attached poly(hydroxyethyl methacrylate) membrane: preparation and properties. J Appl Polym Sci 75(14):1685–1692
23. Akashi M, Takemoto K (1990) New aspects of polymer drugs. Adv Polym Sci 97:107–146
24. Bell CL, Peppas NA (1995) Biomedical membranes from hydrogels and interpolymer complexes. Adv Polym Sci 122:125–175

25. Laporte RJ (1997) Hydrophilic polymer coatings for medical devices. CRC Press, Lancaster, PA
26. Blanco MD, Trigo RM, Garcia O, Teijon JM (1997) Controlled release of cytarabine from poly(2-hydroxyethyl methacrylate-co-N-vinyl-2-pyrrolidone) hydrogels. J Biomater Sci Polym Ed 8(9):709–719
27. Gallardo A, Fernandez F, Bermejo P, Rebuelta M, Cifuentes A, Diez-Masa JC, San Roman J (2000) Controlled release of cyclosporine from VP-HEMA copolymer systems of adjustable resorption monitorized by MEKC. Biomaterials 21(9):915–921
28. Davis TP, Huglin MB (1989) Studies on copolymeric hydrogels of N-vinyl-2-pyrrolidone with 2-hydroxyethyl methacrylate. Macromolecules 22(6):2824–2829
29. Atta AM, Arndt KF (2004) Swelling behaviour of pH- and temperature-sensitive copolymers containing 2-hydroxy-ethyl methacrylate and N-vinyl-2-pyrrolidone crosslinked with new crosslinkers. Polym Int 53(11):1870–1881. doi:10.1002/Pi.1606
30. Zaldivar D, Peniche C, Gallardo A, Sanroman J (1993) Biocompatible hydrogels of controlled hydrophobicity from copolymers of N-vinyl-2-pyrrolidone and furfuryl methacrylate. Biomaterials 14(14):1073–1079
31. Langer R, Cima LG, Tamada JA, Wintermantel E (1990) Future-directions in biomaterials. Biomaterials 11(9):738–745
32. Blanco MD, Trigo RM, Teijon C, Gomez C, Teijon JM (1998) Slow releasing of ara-C from poly(2-hydroxyethyl methacrylate) and poly(2-hydroxyethyl methacrylate-co-N-vinyl-2-pyrrolidone) hydrogels implanted subcutaneously in the back of rats. Biomaterials 19(7–9):861–869
33. Title 21 CFR (Code of Federal Regulations) 175.105 (2010)
34. Mabilleau G, Aguado E, Stancu IC, Cincu C, Basle ME, Chappard D (2008) Effects of FGF-2 release from a hydrogel polymer on bone mass and microarchitecture. Biomaterials 29(11):1593–1600. doi:10.1016/j.biomaterials.2007.12.01
35. Cifuentes A, Diez-Masa JC, Montenegro C, Rebuelta M, Gallardo A, Elvira C, San Roman J (2000) Recombinant growth hormone delivery systems based on vinylpyrrolidone-hydroxyethyl methacrylate copolymer matrices: monitoring optimization by capillary zone electrophoresis. J Biomater Sci Polym Ed 11(9):993–1005
36. Frutos P, Diez-Pena E, Frutos G, Barrales-Rienda JM (2002) Release of gentamicin sulphate from a modified commercial bone cement. Effect of (2-hydroxyethyl methacrylate) comonomer and poly(N-vinyl-2-pyrrolidone) additive on release mechanism and kinetics. Biomaterials 23(18):3787–3797
37. Ahmad B, Bashir S, Nisa SU, Huglin MB (2004) Chemically crosslinked N-vinyl-2-pyrrolidone/2-hydroxyethyl methacrylate (VP/HEMA) copolymer for the controlled release of cyclic oligopeptide. Turk J Chem 28(3):279–285
38. Matsushima S, Takasu A, Inai Y, Hirabayashi T, Era S, Sogami M, Sasaki F, Ohsaki H, Kinosada Y (2002) Equivalent cross-relaxation rate imaging in the synthetic copolymer gels and invasive ductal carcinomas of the breast. Magn Reson Imaging 20(3):285–293
39. Hosaka S, Yamada A, Tanzawa H, Momose T, Magatani H, Nakajima A (1980) Mechanical-properties of the soft contact-lens of poly(methyl methacrylate-N-vinylpyrrolidone). J Biomed Mater Res 14(5):557–566
40. Compan V, Garrido J, Manzanares JA, Andres J, Esteve JS, Lopez ML (1992) True and apparent oxygen permeabilities of contact-lenses. Optom Vis Sci 69(9):685–690
41. Swan MC, Bucknall DG, Goodacre TE, Czernuszka JT (2011) Synthesis and properties of a novel anisotropic self-inflating hydrogel tissue expander. Acta Biomater 7(3):1126–1132. doi:10.1016/j.actbio.2010.10.017
42. Chummun S, Addison P, Stewart KJ (2010) The osmotic tissue expander: a 5-year experience. J Plast Reconstr Aesthet Surg 63(12):2128–2132. doi:10.1016/j.bjps.2010.02.002
43. Obdeijn MC, Nicolai JPA, Werker PMN (2009) The osmotic tissue expander: a three-year clinical experience. J Plast Reconstr Aesthet Surg 62(9):1219–1222. doi:10.1016/j.bjps.2007.12.088
44. von See C, Rucker M, Bormann KH, Gellrich NC (2010) Using a novel self-inflating hydrogel expander for intraoral gingival tissue expansion prior to bone augmentation. Br J Oral Maxillofac Surg 48(4):e5–e6. doi:10.1016/j.bjoms.2009.10.025
45. Gallardo A, Lemus AR, Roman JS, Cifuentes A, Diez-Masa JC (1999) Micellar electrokinetic chromatography applied to copolymer systems with heterogeneous distribution. Macromolecules 32(3):610–617
46. Odian G (2004) Principles of polymerization, 4th edn. Wiley, Hoboken, NJ
47. Dionisio JM, Odriscoll KF (1979) High-conversion co-polymerization of styrene and methyl-methacrylate. J Polym Sci, Part C: Polym Lett 17(11):701–707
48. Elias HG (1997) An introduction to polymer science. VCH, Weinheim
49. Hautus FLM, Linssen HN, German AL (1984) Dependence of computed copolymer reactivity ratios on the calculation method. 1. Effect of experimental setup. J Polym Sci, Part A: Polym Chem 22(11):3487–3498
50. Hamielic AE, MacGregor JF, Pendilis A (1989) Copolymerization comprehensive polymer science. Pergamon, New York
51. Jenkins AD (1996) Reactivity in radical copolymerization. Comprehensive polymer science second supplement. Pergamon Press, New York
52. Faragalla MM, Hill DJT, Whittaker AK (2002) The copolymerization of N-vinyl-2-pyrrolidone with 2-hydroxyethyl methacrylate. Polym Bull 47(5):421–427
53. Alissa MA, Davis TP, Huglin MB, Yip DCF (1985) Copolymerizations involving N-vinyl-2-pyrrolidone. Polymer 26(12):1869–1874
54. Lee SG, Brunello GF, Jang SS, Bucknall DG (2009) Molecular dynamics simulation study of P (VP-co-HEMA) hydrogels: effect of water content on equilibrium structures and mechanical properties. Biomaterials 30(30):6130–6141
55. Lee SG, Brunello GF, Jang SS, Lee JH, Bucknall DG (2009) Effect of monomeric sequence on mechanical properties of P(VP-co-HEMA) hydrogels at low hydration. J Phys Chem B 113(19):6604–6612
56. Lee JH, Bucknall DG (2008) Swelling behavior and network structure of hydrogels synthesized using controlled UV-initiated free radical polymerization. J Polym Sci, Part B: Polym Phys 46(14):1450–1462. doi:10.1002/Polb.21481
57. Jang SS, Goddard WA, Kalani MYS (2007) Mechanical and transport properties of the poly(ethylene oxide)-poly(acrylic acid) double network hydrogel from molecular dynamic simulations. J Phys Chem B 111(7):1729–1737. doi:10.1021/Jp0656330
58. Jang SS, Goddard WA, Kalani MYS, Myung D, Frank CW (2007) Mechanical and transport properties of the poly(ethylene oxide)-poly(acrylic acid) double network hydrogel from molecular dynamic simulations. J Phys Chem B 111(51):14440
59. Brunello G, Lee SG, Jang SS, Qi Y (2009) A molecular dynamics simulation study of hydrated sulfonated poly (Ether Ether Ketone) for application to polymer electrolyte membrane fuel cells: effect of water content. J Renew Sustain Energy 1:033101
60. Jang SS, Goddard WA (2007) Structures and transport properties of hydrated water-soluble dendrimer-grafted polymer membranes for application to polymer electrolyte membrane fuel cells: classical molecular dynamics approach. J Phys Chem C 111(6):2759–2769
61. Jang SS, Lin ST, Cagin T, Molinero V, Goddard WA (2005) Nanophase segregation and water dynamics in the dendrion diblock copolymer formed from the Frechet polyaryl ethereal dendrimer and linear PTFE. J Phys Chem B 109(20):10154–10167. doi:10.1021/Jp050125w

62. Jang SS, Molinero V, Cagin T, Goddard WA (2004) Nanophase-segregation and transport in Nafion 117 from molecular dynamics simulations: effect of monomeric sequence. J Phys Chem B 108(10):3149–3157. doi:10.1021/Jp036842c
63. Mayo SL, Olafson BD, Goddard WA (1990) Dreiding—a generic force-field for molecular simulations. J Phys Chem 94(26):8897–8909
64. Levitt M, Hirshberg M, Sharon R, Laidig KE, Daggett V (1997) Calibration and testing of a water model for simulation of the molecular dynamics of proteins and nucleic acids in solution. J Phys Chem B 101(25):5051–5061
65. Lee SG, Jang SS, Kim J, Kim G (2010) Distribution and diffusion of water in model epoxy molding compound: molecular dynamics simulation approach. IEEE Trans Adv Packag 33(2):333–339. doi:10.1109/Tadvp.2009.2033570
66. Lee SG, Choi JI, Koh W, Jang SS, Kim J, Kim G (2011) Effect of temperature on water molecules in model epoxy molding compound: molecular dynamics simulation approach IEEE transactions on components. Packag Manuf Technol 1(10):1533–1542
67. Brunello GF, Mateker WR, Lee SG, Choi JI, Jang SS (2011) Effect of temperature on structure and water transport of hydrated sulfonated poly (Ether Ether Ketone): a molecular dynamics simulation approach. J Renew Sustain Energy 3:043111
68. Plimpton S (1995) Fast parallel algorithms for short-range molecular-dynamics. J Comput Phys 117(1):1–19
69. Plimpton SJ, Pollock R, Stevens M (1997) Particle-mesh ewald and rRESPA for parallel molecular dynamics simulations. Paper presented at the eighth SIAM conference on parallel processing for scientific computing, Minneapolis, MN
70. Swope WC, Andersen HC, Berens PH, Wilson KR (1982) A computer-simulation method for the calculation of equilibrium-constants for the formation of physical clusters of molecules—application to small water clusters. J Chem Phys 76(1):637–649
71. Hoover WG (1985) Canonical dynamics—equilibrium phase-space distributions. Phys Rev A 31(3):1695–1697
72. Nose S (1984) A unified formulation of the constant temperature molecular-dynamics methods. J Chem Phys 81(1):511–519
73. Nose S, Klein ML (1983) A study of solid and liquid carbon tetrafluoride using the constant pressure molecular-dynamics technique. J Chem Phys 78(11):6928–6939
74. Rappe AK, Goddard WA (1991) Charge equilibration for molecular-dynamics simulations. J Phys Chem 95(8):3358–3363
75. Hockney RW, Eastwood JW (1981) Computer simulation using particles. McGraw-Hill International Book Co., New York
76. Davis TP, Huglin MB (1988) Some mechanical-properties of Poly(2-Hydroxyethyl Methacrylate) gels swollen in water 1,4-Dioxane mixtures. Makromolekulare Chemie-Rapid Communications 9(1):39–43
77. Hong Y, Chirila TV, Cuypers MJH, Constable IJ (1996) Polymers of 1-vinyl-2-pyrrolidinone as potential vitreous substitutes: physical selection. J Biomater Appl 11(2):135–181
78. TakacsNovak K, Avdeef A (1996) Interlaboratory study of log P determination by shake-flask and potentiometric methods. J Pharm Biomed Anal 14(11):1405–1413
79. LOGKOW Databank (1994) Sangster Research Laboratories
80. Kou JH, Amidon GL, Lee PI (1988) Ph-dependent swelling and solute diffusion characteristics of poly(Hydroxyethyl methacrylate-Co-methacrylic acid) hydrogels. Pharm Res 5(9):592–597
81. Khare AR, Peppas NA (1995) Swelling deswelling of anionic copolymer gels. Biomaterials 16(7):559–567
82. Peppas NA, Wright SL (1996) Solute diffusion in poly(vinyl alcohol) poly(acrylic acid) interpenetrating networks. Macromolecules 29(27):8798–8804
83. Russell RJ, Axel AC, Shields KL, Pishko MV (2001) Mass transfer in rapidly photopolymerized poly(ethylene glycol) hydrogels used for chemical sensing. Polymer 42(11):4893–4901
84. Peppas NA, Wright SL (1998) Drug diffusion and binding in ionizable interpenetrating networks from poly(vinyl alcohol) and poly(acrylic acid). Eur J Pharm Biopharm 46(1):15–29
85. Saxton MJ (2001) Anomalous subdiffusion in fluorescence photobleaching recovery: a Monte Carlo study. Biophys J 81(4):2226–2240
86. Weiss M, Elsner M, Kartberg F, Nilsson T (2004) Anomalous subdiffusion is a measure for cytoplasmic crowding in living cells. Biophys J 87(5):3518–3524. doi:10.1529/biophysj.104.044263
87. Schutz GJ, Schindler H, Schmidt T (1997) Single-molecule microscopy on model membranes reveals anomalous diffusion. Biophys J 73(2):1073–1080
88. Weiss M, Hashimoto H, Nilsson T (2003) Anomalous protein diffusion in living cells as seen by fluorescence correlation spectroscopy. Biophys J 84(6):4043–4052
89. Azurmendi HF, Ramia ME (2001) Anomalous diffusion of water in a hydrogel of sucrose and diepoxide monomers. J Chem Phys 114(21):9657–9662
90. Drazer G, Zanette DH (1999) Experimental evidence of power-law trapping-time distributions in porous media. Phys Rev E 60(5):5858–5864
91. Robinson D, Anderson JE, Lin JL (1990) Measurement of diffusion-coefficients of some indoles and ascorbic-acid by flow-injection analysis. J Phys Chem 94(2):1003–1005
92. CRC handbook of chemistry and physics (2005) 85th edn. CRC Press, Boca Raton, FL
93. Gladden JK, Dole M (1953) Diffusion in supersaturated solutions. 2. Glucose solutions. J Am Chem Soc 75(16):3900–3904
94. Ribeiro ACF, Ortona O, Simoes SMN, Santos CIAV, Prazeres PMRA, Valente AJM, Lobo VMM, Burrows HD (2006) Binary mutual diffusion coefficients of aqueous solutions of sucrose, lactose, glucose, and fructose in the temperature range from (298.15 to 328.15) K. J Chem Eng Data 51(5):1836–1840. doi:10.1021/Je0602061
95. Myung D, Koh W, Ko J, Noolandi J, Carrasco M, Smithc A, Frank C, Ta C (2005) Characterization of poly(ethylene glycol)-poly(acrylic acid) (PEG-PAA) double networks designed for corneal implant applications. Investig Ophthalmol Vis Sci 46 (Abstract 5003)
96. Giovambattista N, Debenedetti PG, Rossky PJ (2007) Hydration behavior under confinement by nanoscale surfaces with patterned hydrophobicity and hydrophilicity. J Phys Chem C 111(3):1323–1332. doi:10.1021/Jp065419b
97. BellissentFunel MC, SridiDorbez R, Bosio L (1996) X-ray and neutron scattering studies of the structure of water at a hydrophobic surface. J Chem Phys 104(24):10023–10029